Lessons Learned from Transient Analysis of Combustion Equipment in the Process Industries

Joseph D. Smith, Ph.D., Laufer Endowed Energy Chair
Missouri University of Science and Technology, Rolla, Missouri, USA

Robert E. Jackson, Vikram Sreedharan, Ph.D., Zachary P. Smith and Ahti Suo-Anttila, Ph.D.
Elevated Analytics Consulting, Inc., Provo, Utah, USA

Doug Allen
Zeeco Inc. Broken Arrow, Oklahoma, USA

INTRODUCTION

During gas flare operation, hydrocarbon gas is fed through a flare stack and ignited by a pilot. During the ignition process, flares generally produce significant amounts of smoke (see Figure 1) since enough mixing energy is not available to entrain surrounding air to completely burn the flare gas. Large Multi-Point Ground Flares (MPGF) with hundreds of flare burners arranged in rows and operated in stages pose a significant safety risk during the ignition process (see Figure 2). Given the amount of flare gas discharged to the atmosphere and the transient ignition process for MPGFs, vapor cloud explosions are possible. Ignition of these large flare systems rely on cross lighting between the piloted burner located at the end of each row to operate. This transient cross lighting process relies on transport of highly reactive combustion radicals from the lit burner to an adjacent burner (see Figure 3). The transient ignition and operation of fired equipment has been studied using CFD to assess the safety and environmental issues associated with fired equipment operation. The results of several of these studies will be presented in this paper.

Figure 1 – Flare flame moments after ignition showing black carbon emissions formed during transient ianition

THE CFD COMBUSTION MODEL

The CFD tool used in this work simulates turbulent reaction chemistry coupled with radiative transport between buoyancy driven fires (i.e., pool fires, gas flares, etc.) and surrounding objects (i.e., wind fence, process equipment, etc.). The code provides "reasonably" accurate estimates of various risk scenarios for flare operations including wind speed and direction, % flame coverage, and thermal fatigue for a given geometry. CFD analysis of flares generally can be completed on the order of hours to a few days using a "basic" desktop workstation. For transient combustion analysis, Large Eddy Simulation (LES) is used to describe turbulent reacting flows. The code used in this work was derived from an earlier CFD tool referred to as ISIS-3D [1]. ISIS-3D was initially validated for simulating pool fires [2]. ISIS-3D was commercialized into a new CFD tool called C3d for use to analyze large gas flares. C3d has previously been applied to MPGFs, elevated air-assisted flares, and utility flares with detailed kinetics to describe general hydrocarbon combustion [3], [4]. C3d predicts flame size and shape, smoking potential and radiation flux from flames [5]. C3d simulations of flame height and flame-to-ground radiation have been validated by direct comparison to measured flame size, shape, and radiation measurements taken during single-burner and multi-burner tests conducted under no-wind and low-wind ambient conditions [6].

Figure 2 - Multi-point ground flare contains hundreds of burners

METHODOLOGY

To analyze transient operation of large process heaters, elevated gas flares, MPGFs, and waste incinerators, the transient, LES based Computational Fluid Dynamics model described above was used. Initially, this code was used to model pool fires [2] but more recently has been applied to study wind effects on MPGFs [3], transient ignition of MPGFs [6], and safety issues related to radiation from adjacent MPGFs [7]. The LES based code has also recently been applied to study

Figure 3 - Multi-point flare cross lighting relies on hot-combustion gases (radicals) from the piloted burner to ignite the neighboring burner

wind effects on MPGFs [3], transient ignition of MPGFs [6], and safety issues related to radiation from adjacent MPGFs [7]. The LES based code has also recently been applied to illustrate transient operation of process burners. The work reported in this paper extends previous work which compares LES to RANS based CFD analysis of process burners in a pyrolysis heater [8]. Smith et al., [9] compares LES to RANS based codes for application to industrial combustion equipment to highlight the strengths and weaknesses of steady-state analysis and transient analysis. This previous work showed that transient LES based CFD codes applied to process heaters are best for near-burner analysis. Current Low NOx lean premixed burners often exhibit long lazy (unsteady) flames. Ignition delays of these burners possess another safety risk. Finally, flame flicker in a heater may also alter radiation transfer to the process tubes, which impacts efficiency.

LES based CFD codes are well suited to investigate safety issues related to flare ignition, MPGF cross lighting and transient combustion inside process heaters. The code must describe the turbulent mixing of fuel and oxidizer in a transient fashion coupled with chemical reactions. C3d has been successfully demonstrated for transient combustion process using simplified chemical reaction mechanisms. The following simplified mechanism was used to study transient ignition of an elevated multi-point flare [4]:

$$1\text{kg}\ \boldsymbol{F} + (2.87\text{-}2.6S_1)\ \text{kg}\ \boldsymbol{O_2} \rightarrow \mathbf{S_1}\ \text{kg}\ \boldsymbol{C} + (3.87\text{-}3.6S_1)\ \text{kg}\ \boldsymbol{PC} + (50\text{-}32S_1)\ \text{MJ} \qquad \textbf{\textit{Eq. 1}}$$

$$1\text{kg}\ \boldsymbol{F} + 0.3\ \text{MJ} \rightarrow S_2\ \text{kg}\ \boldsymbol{C} + (1\text{-}S_2)\ \text{kg}\ \boldsymbol{IS} \qquad \textbf{\textit{Eq. 2}}$$

$$1\text{kg } \boldsymbol{C} + 2.6 \text{ kg } \boldsymbol{O_2} \rightarrow 3.6 \text{ kg } \mathbf{CO_2} + 32 \text{ MJ} \qquad \textbf{\textit{Eq. 3}}$$

$$1\text{kg } IS + (2.87 - 2.6S_2)/(1\text{-}S_2) \text{ kg } \boldsymbol{O_2} \rightarrow (3.87 - 3.6S_2)/(1\text{-}S_2) \text{ kg } \mathbf{PC} + (50\text{-}32S_2)/(1\text{-}S_2) \text{ MJ} \qquad \textbf{\textit{Eq. 4}}$$

In this case, the first reaction (Eq. 1) describes the incomplete combustion of hydrocarbon fuel (***F***) with oxygen to produce products of combustion (**PC**) and black carbon (**C**). This reaction produces S_1 kilograms of black carbon per kilogram of fuel consumed. In this case, S_1 depends on the fuel; 0.005 shown to be appropriate by Gao et al. [10] for light hydrocarbons. Reaction 2 (Eq. 2) approximates endothermic fuel pyrolysis cracking which produces S_2 kilograms of black carbon; 0.15 shown appropriate for light hydrocarbons. Reaction 3 (Eq. 3) consumes black carbon and oxygen to produce carbon dioxide and some energy. Reaction 4 (Eq. 4) consumes the Intermediate Species (*IS*) formed in the second reaction with additional oxygen to form more combustion bi-products and energy. These reactions are approximated using the Eddy-Dissipation Concept method originally developed by Magnussen and Hjertager [11] and elsewhere by Smith, et al., [3].

Modified Combustion Model for Ethylene Flares

The combustion model described initially by Said et.al. [10] and described above was used previously for flare analysis by Smith et.al. [3]. As outlined, this model considered Fuel from the flare tip, oxygen from surrounding air, products of combustion produced by complete combustion, soot, and non-radiating intermediate species. Applying the general combustion model to Hydrogen and Ethylene yields:

Combustion Reaction 1:

$$H_2 + 8O_2 \rightarrow 9H_2O + 141\ \mathit{MJ/kg}\ (A=10^{15},\ T_A=10{,}500\text{K}) \qquad \textbf{\textit{Eq. 5}}$$

Combustion Reaction 2:

$$CO + 0.57[O_2]^{1/2} + 0.64[H_2O]^{1/2} \rightarrow 1.57CO_2 + 0.64H_2O + 10.1\ \mathit{MJ/kg}\ (A=10^{13},\ T_A=15{,}151\text{K}) \qquad \textbf{\textit{Eq.6}}$$

Combustion Reaction 3:

$$[C_2H_4]^{1/2} + 0.769O_2 \rightarrow 0.769H_2O + 0.801C_2H_2 + 11.5\ \mathit{MJ/kg}\ (A=10^{15},\ T_A=10{,}500\text{K}) \qquad \textbf{\textit{Eq. 7}}$$

Combustion Reaction 4:

$$[C_2H_2]^{1/2} + 2.46O_2 \rightarrow + 2.62CO_2 + 0.588H_2O + 0.3\ \text{Soot} + 29.2\ \mathit{MJ/kg}\ (A=10^{15},\ T_A=15{,}500\text{K}) \qquad \textbf{\textit{Eq. 8}}$$

Combustion Reaction 5:

$$\text{Soot} + 1.33O_2 \rightarrow 2.33CO + 13.6\ \mathit{MJ/kg}\ (A=10^{15},\ T_A=13{,}590\text{K}) \qquad \textbf{\textit{Eq. 9}}$$

with coefficients selected to consume all the soot and intermediate products so the same amount of species and thermal energy as direct combustion of the fuel would produce. The coefficients in these reactions were written on a mass basis (kilograms of reactant). In previous applications of this combustion model [3] [4], the flare gas Arrhenius combustion time scale (kinetics) was combined with the turbulence eddy breakup time scale (mixing) to yield an overall time scale for the reaction rate:

$$t_{total} = t_{arrhenius} + t_{turb} = \frac{1}{C_i} = \frac{1}{\boldsymbol{A_k T^b} exp^{-\left(\frac{\boldsymbol{T_A}}{\boldsymbol{T}}\right)}} + \frac{C_{eb}\Delta x^2}{\varepsilon_{diff}} \qquad \textbf{\textit{Eq.10}}$$

where $\boldsymbol{A_k}$ is the pre exponential coefficient, $\boldsymbol{T_A}$ is an activation temperature, $\boldsymbol{T}$ is the local gas temperature, and $\boldsymbol{b}$ is a global exponent, $\boldsymbol{\Delta x}$ is the characteristic cell size, $\boldsymbol{C_{eb}}$ is a user input constant (~0.2E-04) that is cell size dependent, $\boldsymbol{\varepsilon_{diff}}$ is the eddy diffusivity from the turbulence model, and $\boldsymbol{t_{turb}}$ is the turbulence time scale, i.e. characteristic time required to mix all contents of a computational cell. The reaction rates are combined by simple addition of the time scales. Depending on the kinetics vs. mixing time scales, the characteristic time for each reaction can be different. Thus, the simplified combustion model approximates turbulent reacting flow using the eddy dissipation concept (mixing) with the local equivalence ratio effects (mixing). The Arrhenius kinetics and turbulent mixing approach are similar to the commonly used Eddy-Breakup (EBU) type combustion model and is comparable to more complex PDF based models summarized by Zhang [12].

A minimum number of other irreversible chemical reactions describing the combustion chemistry are required to fulfill the requirements of total energy yield and species consumption and production. Details of the chemical reactions are not critical if oxygen consumption is balanced for the selected fuel and soot produced is calibrated to experimental data. For the fuels selected, a multi-step reaction model for ethylene combustion approximated the global reaction mechanism:

$$^{dX_i}\!/_{dt} = C_i X_1^c X_2^d \qquad \textbf{\textit{Eq. 7}}$$

where X_i is the mole fraction of the rate equation for the ith reaction, C_i is the global reaction rate (*Eq*. 10), and $\boldsymbol{c}$ and $\boldsymbol{d}$ are global exponents. All rate equations are solved simultaneously for each reaction and the stoichiometric coefficients in *Eqs*. 5-9 are used as constraints that couple the equations and insure conservation of energy and chemical species.

Sometimes CFD simulations of turbulent reacting flow uses a single global reaction with required coefficients and powers fit to specific experimental data. In general, this simplified approach is misleading because the coefficients were originally fit to experimental data from a specific combustion experiment. Since it is well known that simulations are sensitive to the computational mesh and specific experimental data, different reaction coefficients are required for a different computational grid.

For the original work reported by Smith *et.al.*, [4] was based on the original work of Duterque *et. al.* [13] and Kim [14] but was adjusted for turbulent mixing conditions since the original work was based on "laminar" flame speed data. Reaction rates were adjusted to match measured combustion data by varying the pre-exponential coefficients to develop a validated combustion model.

Turbulent mixing was accounted for using a proportionality coefficient and cell size factor to match previous flare testing with ethylene. This approach provided a validated combustion model for the reported work as shown in Figure 4.

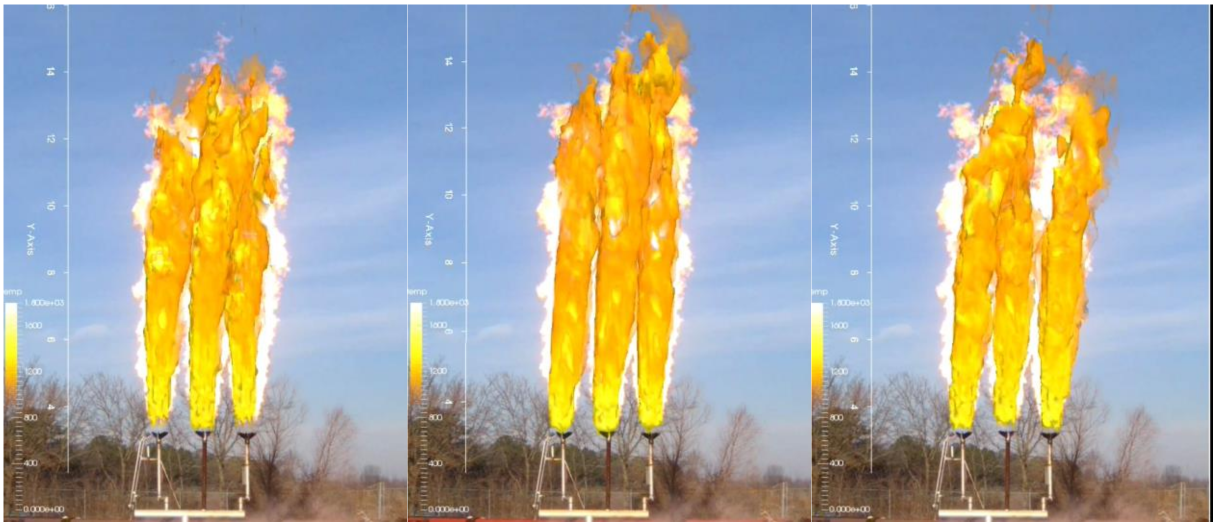

Figure 4 - Comparison of predicted and measured flame shape for a 3-Flare Test burning ethylene gas [15]

ANALYSES OF TRANSIENT IGNITION PROCESSES

The ignition process in fired equipment involves transient chemical reactions between fuel and oxidizer. When a burner is ignited, fuel and air must efficiently mix, or they react incompletely, and produce excess emissions. The resulting unstable flame can lead to unsafe operating conditions.

<u>**Elevated Multi-Point Flare Ignition**</u>

The application was described by Smith et.al. at the 2010 AFRC meeting [4] is summarized below to illustrate the need for transient simulations. As mentioned earlier, flare ignition results in excess smoke during the ignition process since the flare gas fed through the flare tip does not possess enough mixing energy to entrain surrounding air. The multi-point elevated flare in this analysis was designed to fire hundreds of tons of flare gas per hour through multiple tips. When this flare gas ignited it generated a large fireball (see a) with an associated pressure wave. The purpose of this work was to assess the risk of using a manual ignition system (i.e., a flaming arrow shot by an operator into the assumed flare gas plume) which was likely to have an ignition delay.

a)

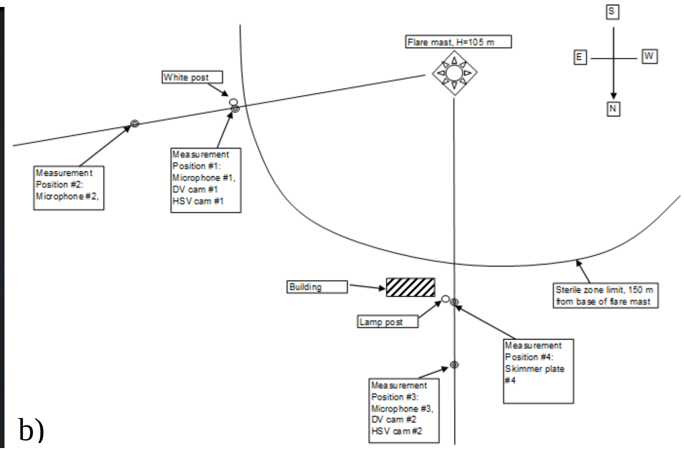

b)

Figure 5 - Elevated Multi-point flare: a) fireball generated during ignition process, b) experimental setup to measure pressure wave generated during the ignition process

To estimate the intensity of the pressure wave, C3d was used to analyze this phenomenon. The computational domain where the flare gas was fed from the nozzles was approximately 3.35 m square (based on flare dimensions) with the computational domain extending approximately 9m above the edge of the flare domain. The bottom of the computational domain was taken as the nozzle top. The overall domain was divided into two regions with the first region, located just above the flare tips, included equal spaced rectangular cells. A second region used variable size cells ranging from 0.05m square cells at the nozzle exit to 0.14m cells at the domain top. The "high resolution" mesh was in the central region of the domain with 80 x 80 x 90 (576,000) cells. The upper region surrounded the lower region with a mesh composed of coarse, highly stretched cells that provided a buffer region to the actual domain boundary. The overall two-zone mesh used a total of 108 x 108 x 102 = 1,189,728 computational cells.

The methodology used to simulate the flare and its nearby surroundings involved running several C3d cases to find the "best" parameter values to match predictions to experimental test data. Once the model was optimized, it was used to estimate the pressure wave emanating from the flare for different flow conditions.

The collection of nozzles included in the overall flare tip were modeled by approximating them using the constant velocity cone formed when a highspeed jet enters an ambient environment. For this approximation, the nozzle tip is represented as a constant velocity cone where flare gas was injected into the domain. The nozzle cone was surrounded by a surface where air was injected into the domain and mixed with the flare gas injected through the nozzle cone (see Figure 6). Since the computational cell size in the nozzle region was nearly the size as the nozzle diameter, injection through the nozzles was approximated by several mass sources located on the nozzle cone surface. A FORTRAN program was written to establish the location of several mass sources on the cone surface. It was determined that to properly model the nozzle properly required approximately 7,700 mass sources through which flare gas was injected at the correct inlet velocity and mass flow rate to model the nozzle as if a very fine computational mesh was used. This approach was used for all nozzles so that the flow was identical for all nozzles. This represents the assumption that no flow mal-distribution between individual nozzles existed.

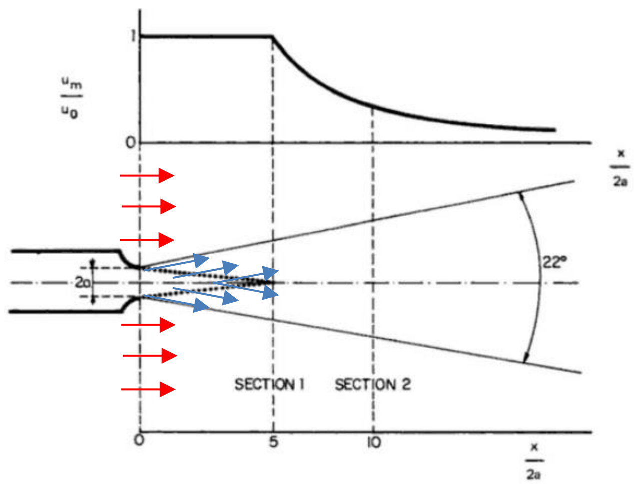

Figure 6 – Use of a free jet discharging into a calm atmosphere – the region outlined by dots is a constant velocity cone which extends 5 nozzle diameters. This approximation was used in length.

The total gas that was injected was adjusted to provide the specified flow for the operating case considered. For this project, flare gas flow rates between 350 – 1,200 Tons/hr (TPH) were considered.

To minimize the computation requirements, chemical reactions for the combustion model were selected to match the total energy yield and species consumption and production. For this work, global reaction mechanisms were picked as starting points [13], [14]. The pre-exponential coefficients (A_k) for the kinetic reaction rate constant was varied with the activation temperature and mole fraction exponents held constant since these were not sensitive to mesh structure. Also, the scale factor that relates turbulence intensity to local strain rate (ε) and the time delay factor that accounts for mixing delay in a computational cell (δ) were varied to optimize the global reaction. Table 1 lists values for the tuning parameters used to optimize the combustion model to meet the data provided for this analysis.

Table 1- Parameters varied in Combustion Modeling tuning

Combustion Model Parameters	Values Considered in Model Tuning
A_k	1.0e14, 2.5e14, 5.0e14, 1.0e15,.,.,.5.0e17
ε	0.10, 0.15, 0.20, 0.25, 0.30, 0.35, 0.40
δ	1.0e-4, 5.0e-5, 1.0e-5, 5.0e-6, 1.0e-6

Other parameters adjusted in this study included: 1) computational grid dimension, 2) turbulence model used (either zero equation and one-equation LES), 3) order of numerical upwind differencing scheme used, and 5) Ignition delay time. With tuned parameters, the CFD model was used to simulate flare ignition with and without ignition delay. Results for the 250ms delay case showed a growing fireball evolving above the tip with the associated pressure wave created by the flame expansion (see Figure 7).

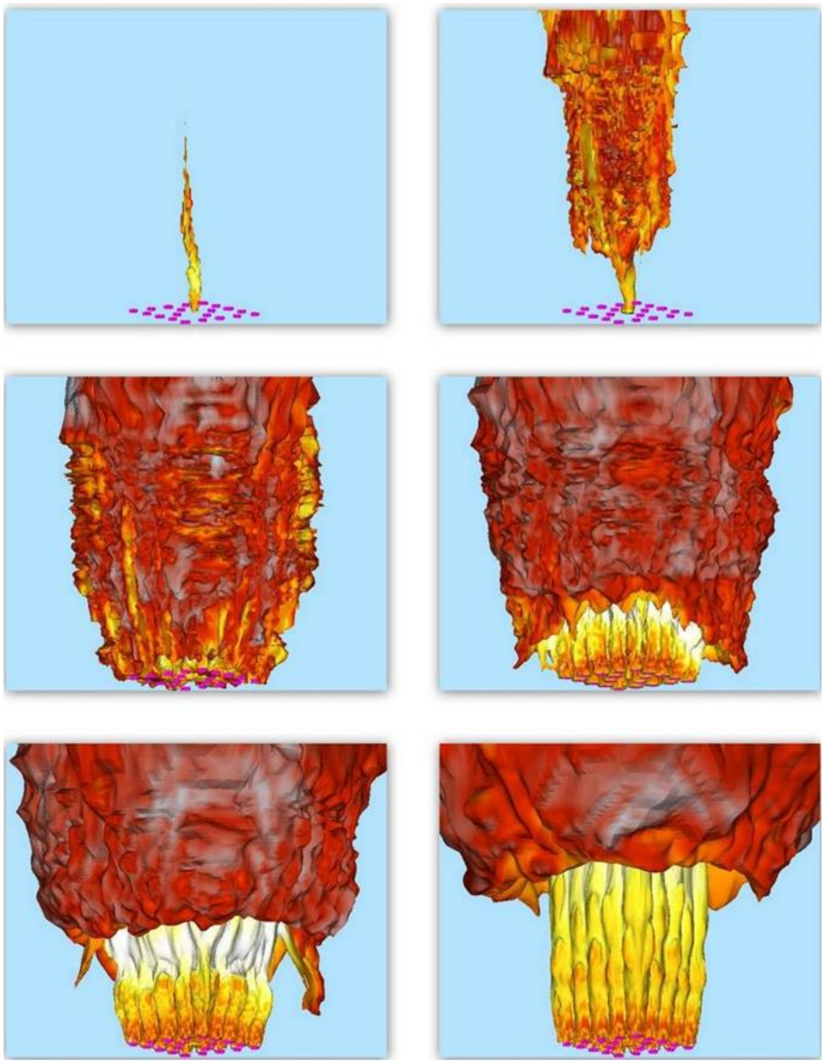

Figure 7 - Growing fireball during elevated flare ignition with 250 ms ignition delay

The pressure wave generated during this case was measured using the experimental setup shown above (see b). For this study, the impact of a 250ms delay was compared to a case without any ignition delay. The pressure wave for the no-delay case was < 100 mbar while the pressure wave for the 250ms delay was > 3000 mbar (see Figure 8).

The lessons learned from this analysis was how important ignition delay can be for an elevated gas flare. The pressure wave created by a short delay caused by using outdated equipment could be catastrophic. This issue would not have been correctly identified using a steady-state RANS based CFD analysis. Based on the results of this study, the client re-examined their design basis for gas flare ignition systems. These results also underscore the importance of the API recommended practice to always have a continuous pilot in operation for all large gas flares.

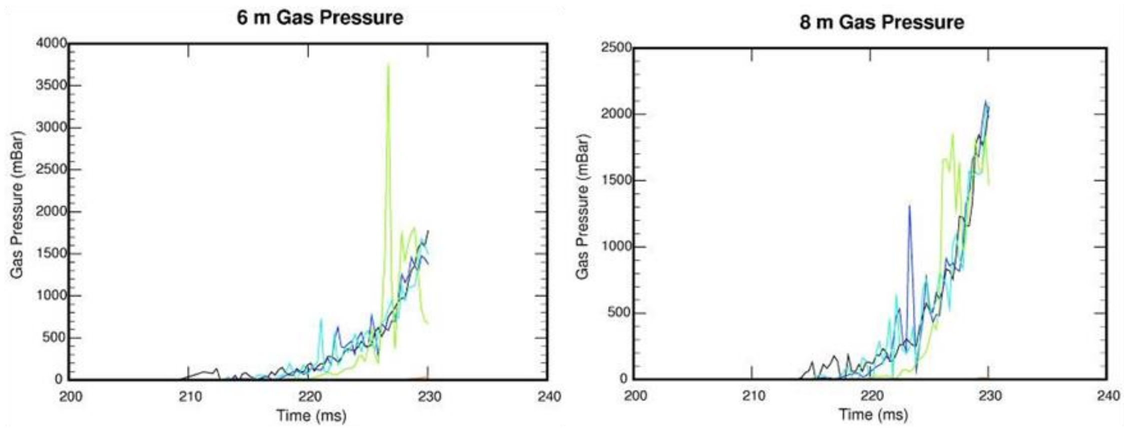

Figure 8 - Pressure around an elevated multi-tip flare with a 250 ms ignition delay

<u>Multi-Point Flare Ignition</u>

Multi-point ground flares are normally used to process large quantities of hydrocarbon gases generated in chemical processing or petrochemical refining. These flares employ hundreds of flare burners oriented in a staggered configuration along feed lines and operated in a staged fashion. A wind fence is included to protect the fire from ambient wind and support high efficiency combustion (see Figure 9). Significant safety concerns of high radiation flux to surrounding personnel and equipment, vapor cloud explosions related to ignition cross lighting, and excessive emissions produced during non-standard operation require detailed analysis before construction and operation [6].

Vapor-cloud explosions of excess hydrocarbons emitted to the atmosphere during the cross-lighting ignition step can produce a significant pressure wave which could damage nearby equipment and workers. In a recent study, it was found that a 0.2-psi pressure wave was possible when a multi-field MPGF experienced as little as a 150ms ignition delay. Staged operations are used to mitigate this safety risk.

A large vapor cloud has the potential to create sizable overpressures which can injure personnel and damage equipment. In order to calculate the potential overpressures a new ignition model was added to *C3d* that simulates the propagation of a combustion/deflagration wave. The new ignition model is based upon a user input propagation speed, which is the minimum velocity that a deflagration wave would have. *C3d* will propagate the deflagration wave through the vapor cloud at this speed or greater. After a computational cell is burning (due to passage of deflagration wave) the code resorts to the kinetics model described earlier in *Eqs.* 1-7. The speed of the deflagration wave at a minimum is the user input speed. However, when the vapor cloud is large enough the hot gas expansion can cause adjacent computational cells to ignite at a time scale shorter than the propagation velocity. In this way flame acceleration occurs, and was found to occur in a number of test cases where the input propagation velocity was large ~100m/s. The deflagration velocity was set by values found in the literature for ethylene (20 - 40m/s) for unobstructed large clouds. This velocity was observed for large lenticular shaped balloons (~10m length) of ethylene gas. Higher propagation velocities such as those for hydrogen (100m/s) would often result in large overpressures (a fraction of an atmosphere) at the MPFG wind fence boundary due to flame acceleration.

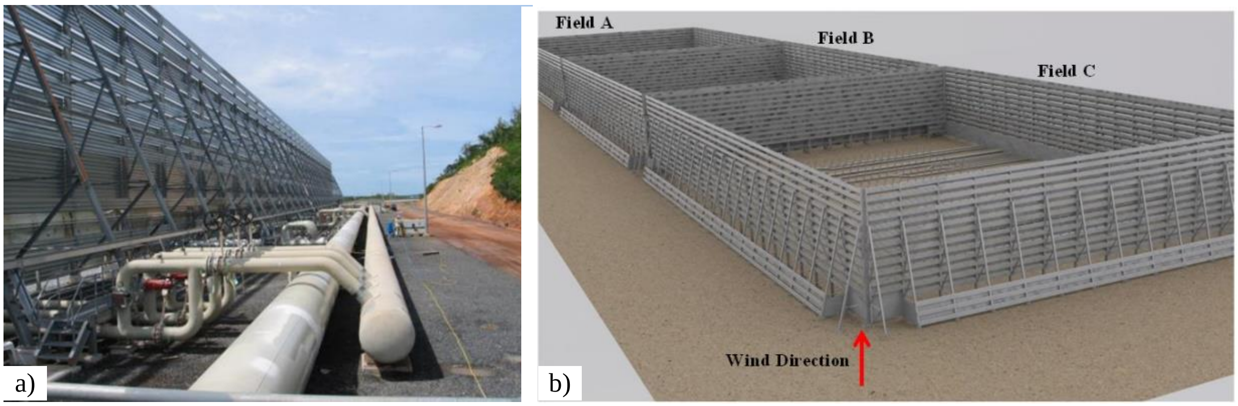

Figure 9 - Large MPGF with: a) staging header and b) a surrounding wind fence for a multi-field flare system

As shown, transient ignition of gas flares creates significant safety concerns related to vapor-cloud explosions which may occur when large amounts of flammable gas are discharged from a flare and ignition is delayed. Depending on local wind conditions (speed and direction) and the flare ignition system, burner-to-burner interaction and burner-to-wind fence interaction may increase or decrease these safety concerns. Flare tip spacing in MPGFs controls how effective transient cross-lighting of a MPGF is which impacts the safety concern.

In a recent study, a MPGF was analyzed using C3d (described earlier) to analyze a multi-field MPGF operated as part of a chemical production plant located on the gulf coast of the United States. This multi-field MPGF system can operate each field individually or all fields simultaneously (see Figure 10). Several operating scenarios considering each field operating individually or combined under various wind conditions and with different flare gas flows were analyzed to assess the safety risks associated with cross-lighting. Of special interest was the safe operation of the largest of the three flare fields referred to as the Ethylene flare. This field is approximately 430’ long by 280’ wide with 19 stages containing 756 tips capable of processing more than 4 million pounds per hour (lb/hr) of light hydrocarbons mixed with hydrogen and inerts (average flare gas MW= 22-25). The safety risk considered in this analysis was the potential impact the pressure wave created by ignition delay of this flare might have on surrounding structures and personnel.

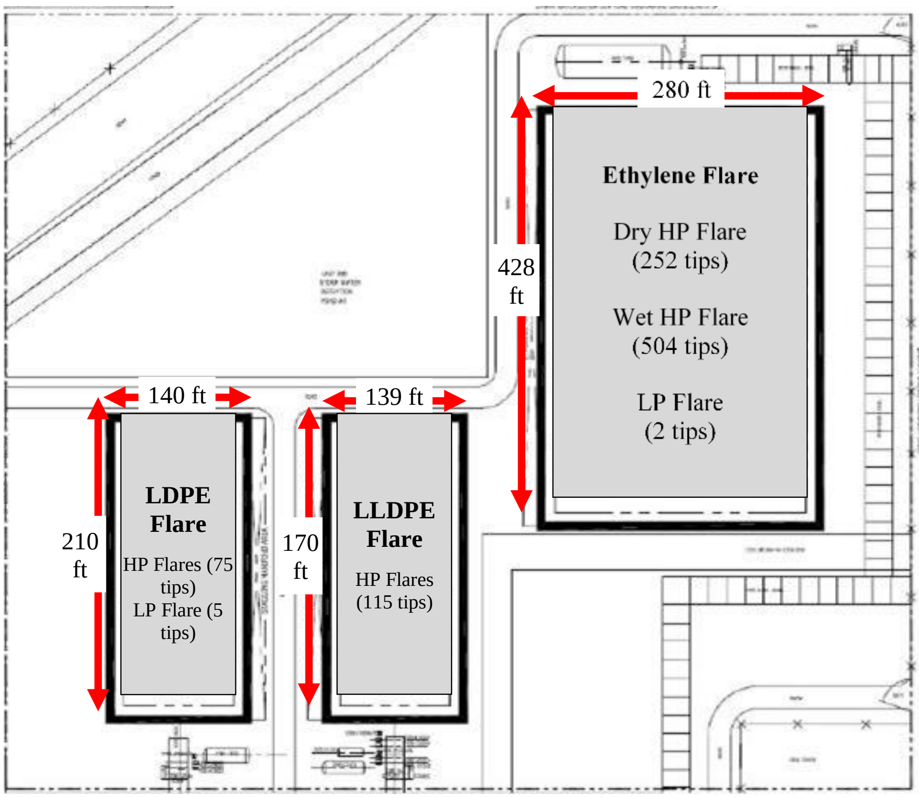

Figure 10 - Plan view of multi-field MPGF showing ethylene field and structures included in CFD analysis

C3d predictions were made for maximum flow conditions with several wind condition to assess the potential of creating an unsafe over-pressure caused by a 150ms ignition delay. The surrounding wind fence, designed to minimize wind effects on the flare flame, affects airflow inside the flare field which also affects ignition performance. Hence, all CFD analyses were done considering the full geometry to include potential effects on ignition.

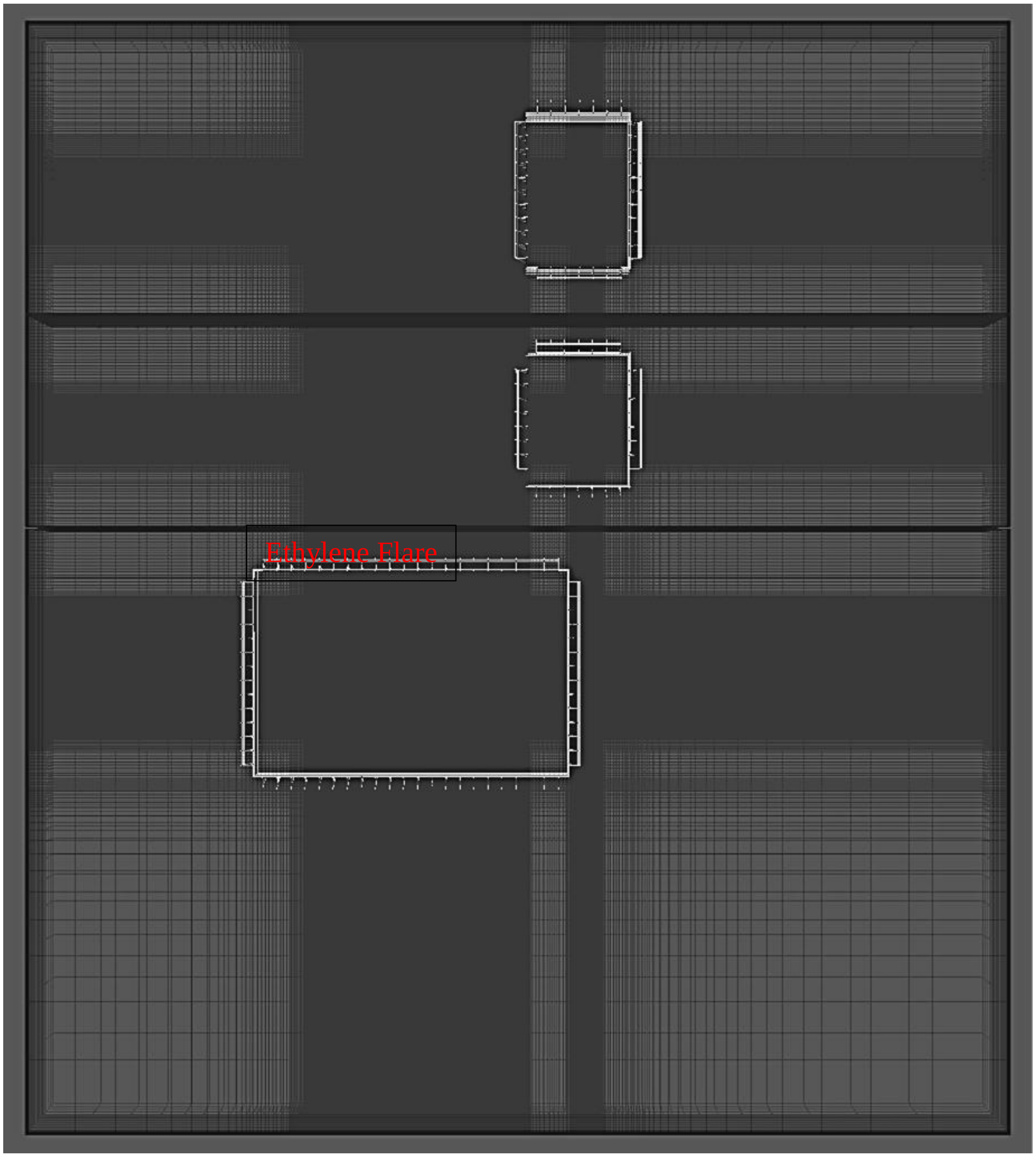

Figure 11 –MPGF geometry all 3 flares included (overlaid on mesh with 11.5 million structured cells)

To reduce computational demand for this analysis, the wind fence was approximated as a porous region to match airflow through the fence to include the wind's impact on flare ignition as originally discussed by Smith et.al. [15]. The overall flare system was approximated using a structured mesh (see Figure 11) which was refined several times to improve simulation results. The final mesh for the total flare system consisted of 11.5 million hexahedral cells refined around the burner tips in each flare field.

This analysis predicted the over-pressure wave created when ignition was delayed by 150ms. Cross lighting scenarios examined a 20 mile per hour wind blowing both perpendicular and parallel to the burner row (see Figure 12). As discussed earlier, short ignition delays result in significant over pressure conditions, which can lead to significant damage to nearby equipment and structures as well as plant personnel working in the vicinity. Although the results from this analysis have a low probability of occurring, this work is one-way MPGF operators can reduce insurance risks associated with their operations.

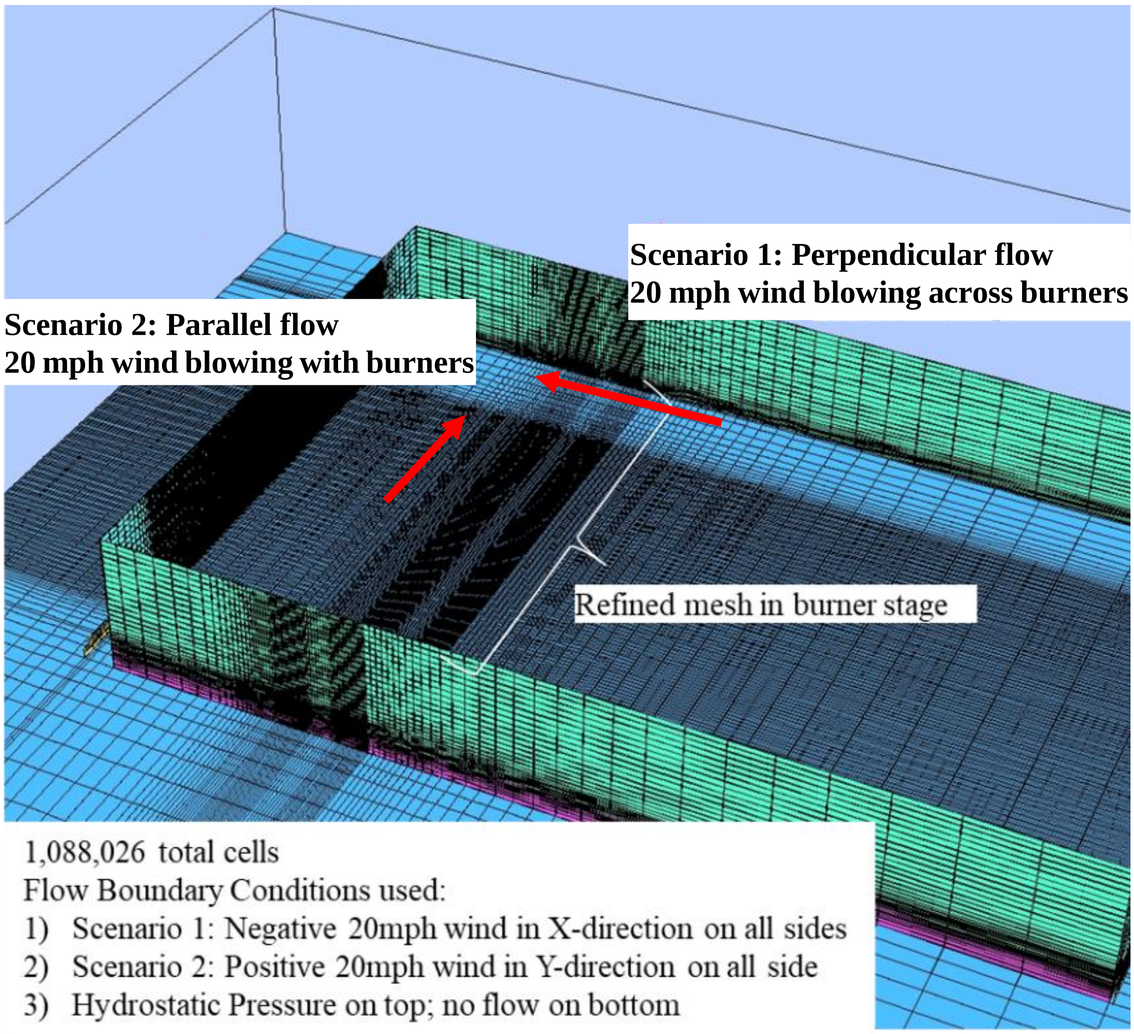

Figure 12 - Computational mesh of Ethylene flare with boundary conditions

The first scenario considered stages 1-4 burning when stage 5 is activated without a pilot allowing unburnt flare gas to vent into the atmosphere. Nearly 800,000 lb/hr is fed to the flare with a 20mph wind blowing in the positive X-direction (see Figure 13). This unburnt gas results in an ethylene plume which disperses above the flare tips and is subject to the cross-wind blowing perpendicular from the lit tips to the unburnt gas plume. In this case, the ethylene plume disperses as shown just before the plume ignites. Flames above the tips in Stages 1-4 (included in a single row) are illustrated as ethylene iso-surfaces colored by temperature. Combustion products, responsible for igniting the adjacent row of burners, are shown above the flames as transparent yellow iso-surfaces. The non-burning tips in Stage 5 (also included in a single row) have unburnt ethylene plumes above the tips shown as blue iso-surfaces. The transparent flames illustrate hot combustion by-products that cross-light the unlit ethylene plume. This analysis was performed to show how large the unignited flammable plume would grow before it ignited and how large a pressure wave would be created when ignition occurred. The predicted pressure wave for this scenario reaches a maximum of 1,400 pascals (0.2 psi) as shown earlier in Figure 14.

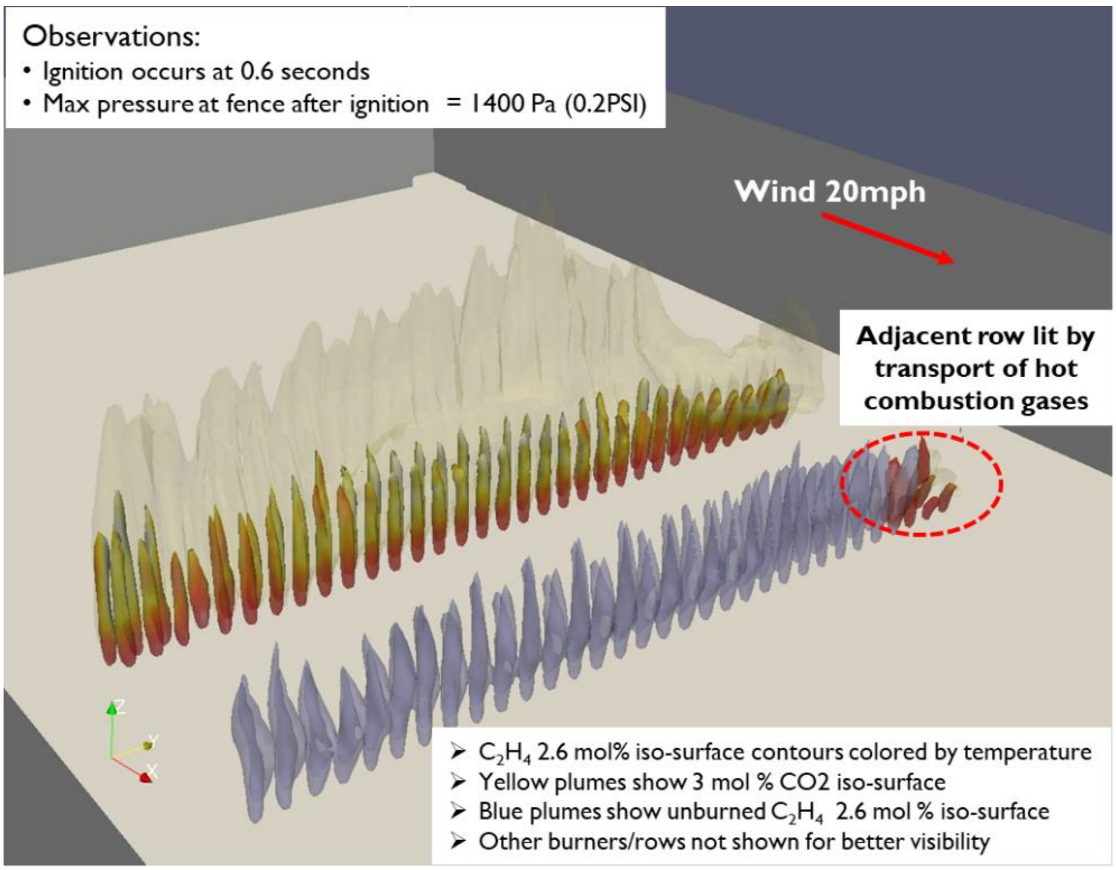

Figure 13 - MPGF ignition test with perpendicular cross wind blowing at 20mph from lit row to unlit row

The second MPGF ignition scenario has the same flare gas flowrate and composition, the same number of stages lit and unlit but assumes a 20mph wind blowing parallel to the flare burners (see Figure 15). As shown, the unignited tips create a larger plume before because hot combustion gases are transported mainly by diffusion this time instead of being convected from the lit tips to the unignited plume. This results in a longer ignition delay (3.6 seconds vs 0.6 seconds) and a

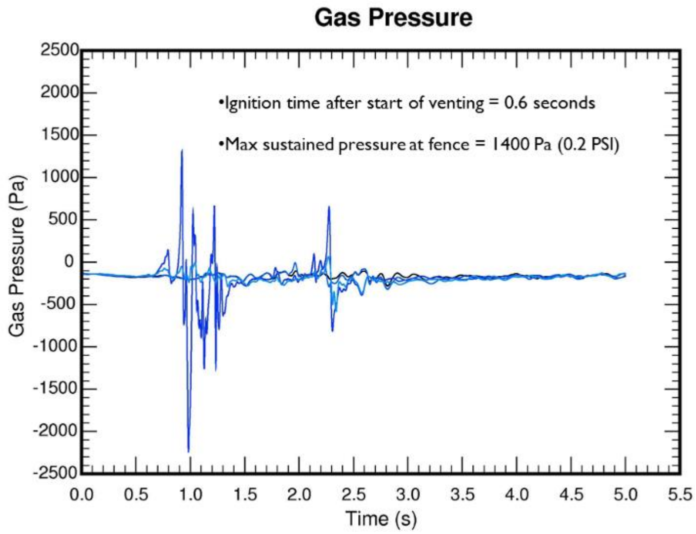

Figure 14 - Pressure wave generated during a MPGF ignition with a 150 ms delay

smaller pressure wave (100 pascals vs 1,400 pascals) as shown in Figure 16. A key observation is that the unlit tips ignite the adjacent ethylene plume part way up the plume. This "cross-lighting" behavior is the same as shown earlier in Figure 3 which is thought to be the cause for a longer ignition delay with a smaller pressure wave. This observed behavior probably means that the flare ignition process is slower and less intense for when the cross wind is parallel to the rows so hot combustion gases must diffusion to adjacent rows to ignite them.

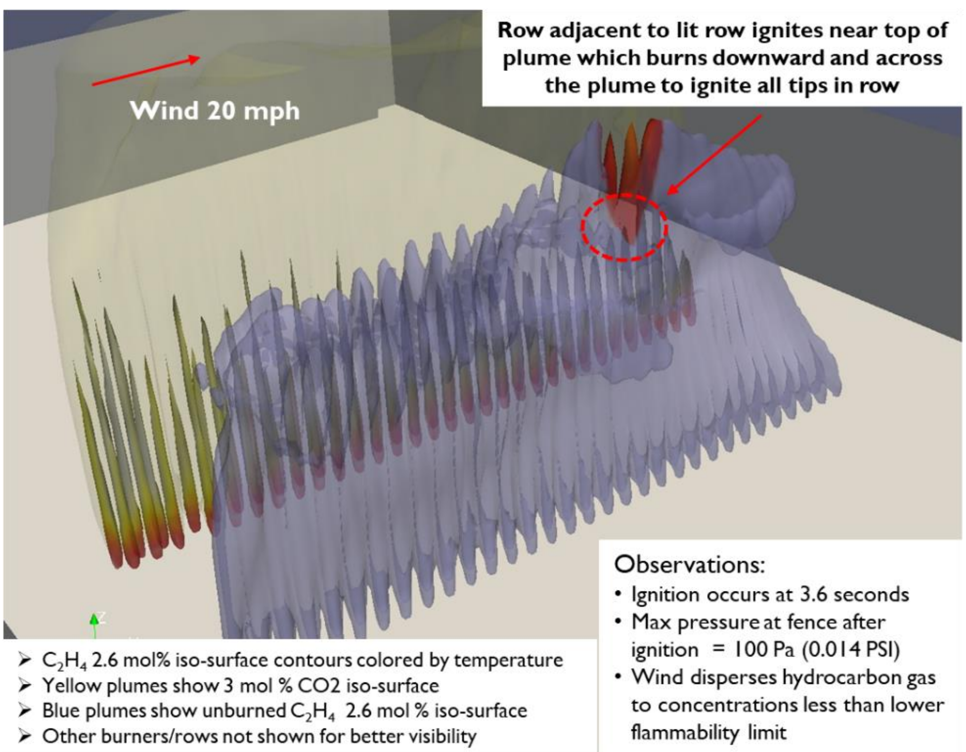

Figure 15- MPGF ignition test with 20mph parallel cross wind

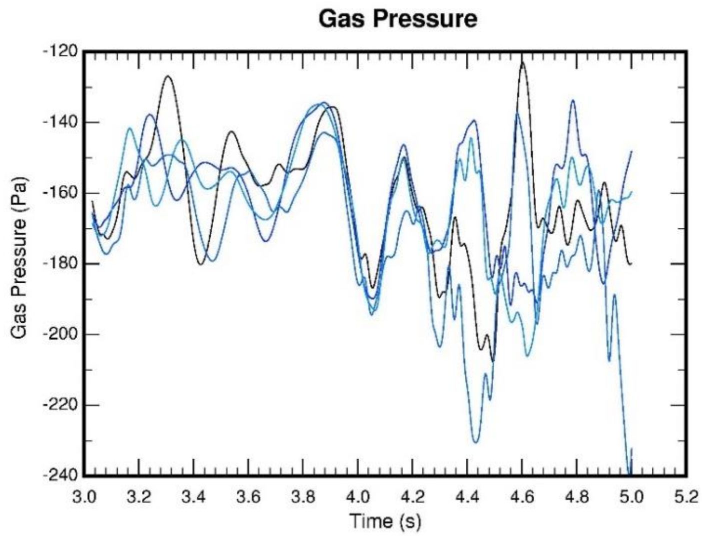

Figure 16 - Pressure wave created with ignition under a 20mph wind blowing parallel to the lit row

Transient Process Burner Operation

Transient operation of process heaters used in the chemical and petro-chemical process industries represents another significant operational challenge. A typical cabin style process heater may contain many individual process burners, each which must be lit and remain lit during heater startup and operation. Advanced low emission burners typically operate in a lean premixed condition, so the flame is stretched out and cooler to reduce NOx emissions (see Figure 17).

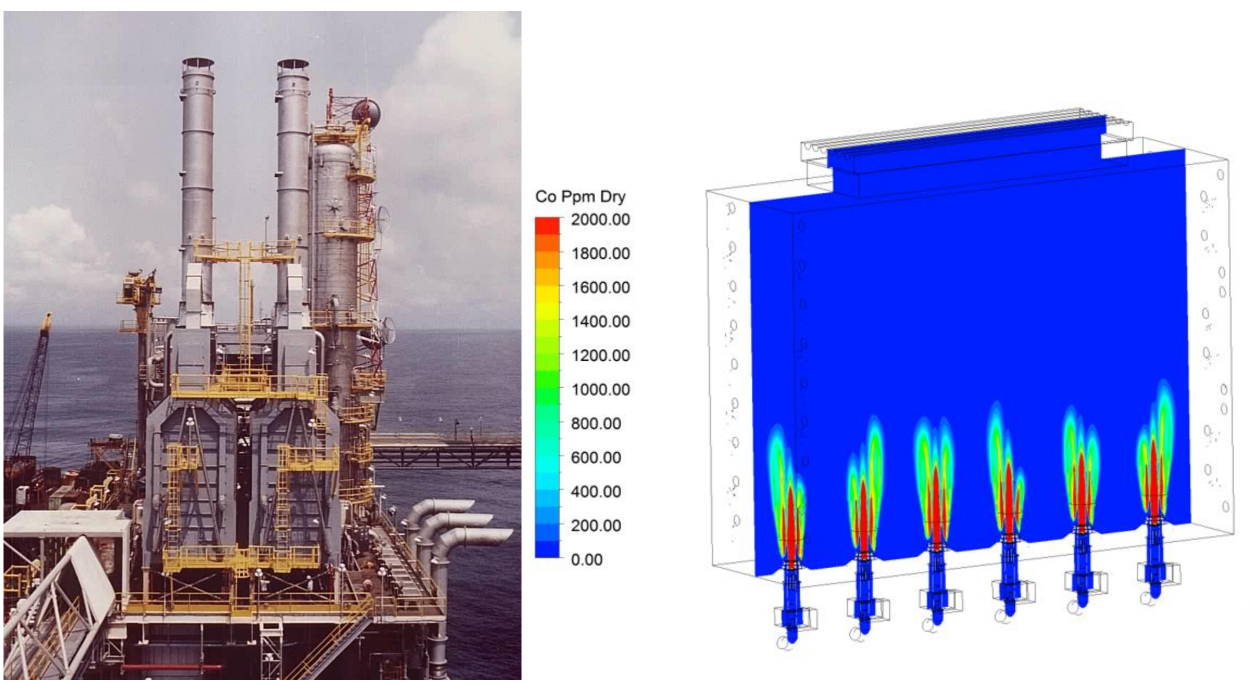

Figure 17 - Cabin Furnace with multi-burner operation

During normal operation, Low-emission burner flames are more affected by furnace currents which can extinguish the flame allowing fuel gas to collect in one region of the furnace box. With oxygen from another part of the furnace transported to the fuel rich region, a large flame may result creating a over-pressure condition in the furnace box that disrupts steady operation, leads to non-optimal performance and can even damage process tubes in the convection section above the furnace box.

This phenomenon was analyzed by varying the air fed to one burner in a sample furnace box shown below (see Figure 18). As shown, during normal operation (LHS image) the flames are uniform in size but when air to one burner is shutoff the flame goes out, but fuel gas continues to be fed from the burner to the furnace box. When air to this burner is turned back on the flame reaches twice the size of the other flames which creates a non-uniform heat flux profile to the process tubes and generate a pressure wave inside the furnace box that flows upward into the convection section putting excess stress on the convection tubes and stack. During heater startup, excess fuel in the furnace box can lead to as a “hard-light off” which furnace operators know from experience. Transient burner operation creates safety hazards, can lead to excess emissions generated and even damage the heater.

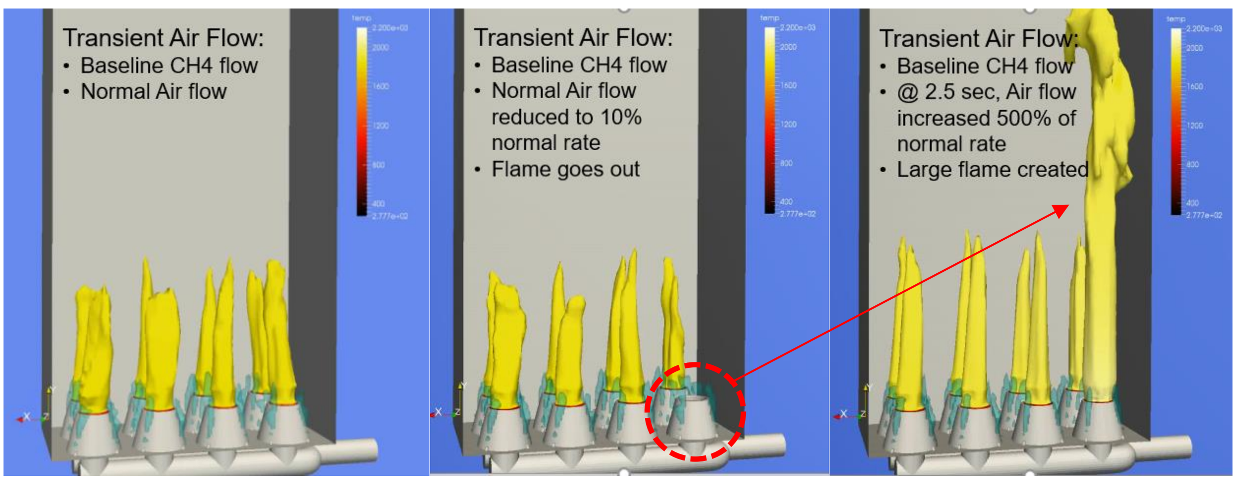

Figure 18 - Transient air flow fed to process burner can create overpressure condition in heater

As mentioned above, non-uniform burner operation with associated “non-steady” flames may also reduce furnace efficiency by altering the thermal flux profile on the process tubes. As reported by Smith, et al., [16] testing in a pyrolysis furnace with different burner configuration changed the measured flux profile (see Figure 19).

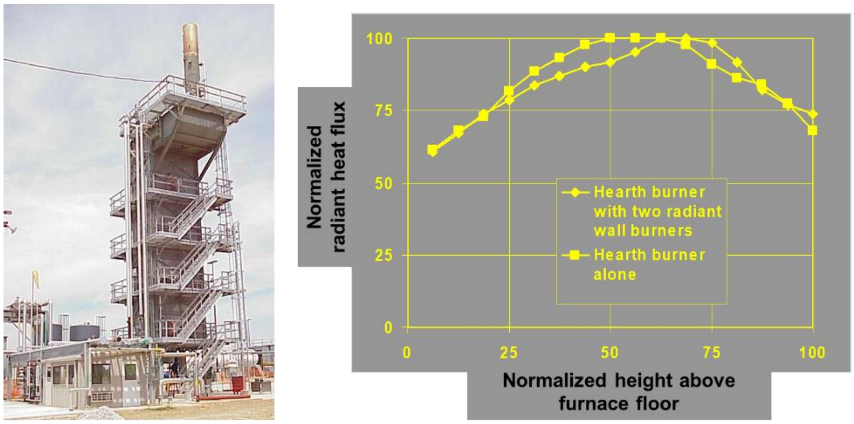

Figure 19 - Heat flux profiles in a pyrolysis furnace with and without wall burners [16]

Normal burner analysis in process heaters has been done assuming steady-state operation as discussed by Smith, et al., [9]. Earlier, the following statement may have been true: "*LES simulations of full combustion furnaces remain rare due to the significant computational requirements and because industry has yet to determine if the costs associated with LES simulation are justified based on the value of the business risk reduction achieved by running such a simulation.*" Today's CFD tools, such as C3d, are available and can be used to perform engineering analysis of transient furnaces operation to explore the impact of non-steady phenomena such as safety issues related to ignition and process efficiency related to flickering flames. Although significant work reported in the literature describing the analyses of transient flare operation, C3d can now be used to analyze non-steady process heater operation as well.

SUMMARY AND CONCLUSIONS

The present work has focused on conducting transient analysis of several different types of process equipment including an elevated multi-point flare, a multi-point ground flare and low emission burners inside a process heater. Each of these studies show how important the transient phenomena is related to safe and efficient operation. The CFD code C3d, previously introduced and discussed in earlier work, has been applied in each of these three case studies to illustrate the feasibility to conduct full transient analysis of very complex processes.

Of specific interest in this paper is the application of C3d to address specific safety related issues of Elevated and Ground flares. Though not in the public domain, C3d is also applicable to analyzing process burner operation to reduce hazardous operation and improve process efficiency.

Based on this work, it is recommended that the C3d code and approaches described herein be applied to other transient problems including refractory cooling in hazardous waste incinerators. Another application may be analyzing transient flame behavior inside a pyrolysis furnace where flow instabilities may accelerate enhance mechanical fatigue and/or flame instabilities may impact thermal fatigue in process tubes. This code should be applied to analyze low-NOx burner operation to assess the impact that non-steady light off may have on emissions control. Finally, it is recommended that the LES based code, C3d, be applied to evaluate various API safety guidelines to confirm or extend the safe operating envelop.

REFERENCES

[1] A. Suo-Anttila, K. Wagner and M. Greiner, "Analysis of Enclosure Fires Using the ISIS-3D CFD Engineering Analysis Code," in *Proceedings of ICONE12, 12th International Conference on Nuclear Engineering*, Arlington, Virginia, April 25-29, 2004.

[2] M. Greiner and A. Suo-Anttila, "Validation of the ISIS Computer Code for Simulating Large Pool Fires Under a Varity of Wind Conditions," *ASME J. Pressure Vessel Technology,* vol. 126, pp. 360-368, 2004.

[3] J. Smith, A. Suo-Anttila, S. Smith and J. Modi, "Evaluation of the Air-Demand, Flame Height, and Radiation Load on the Wind Fence of a Low-Profile Flare Using ISIS-3D,”," in *AFRC-JFRC 2007 Joint International Combustion Symposium*, Marriott Waikoloa Beach Resort, Hawaii, October 21-24, (2007).

[4] J. Smith, A. Suo-Anttila, N. Philpott and S. Smith, "Prediction and Measurement of Multi-Tip Flare Ignition," Sheraton Maui, Hawaii - SepteSheraton Maui, Hawaii, September 26 – 29 (2010).

[5] A. Suo-Anttila and J. Smith, "Application of ISIS Computer Code to Gas Flares Under Varying Wind Conditions," in *2006 American Flame Research Committee International Symposium*, Houston, Texas, October 16-18, 2006.

[6] J. Smith, Jackson, R.E., Z. Smith, D. Allen and S. Smith, "Transient Ignition of Multi-Tip Ground Flares," University of Utah, Salt Lake City, Utah, September 17- 19 (2018).

[7] J. Smith, R. Jackson, V. Sreedharan, A. Suo-Anttila, Z. Smith, D. Allen, D. DeShazer and S. Smith, "Safe Operation of Adjacent Multi-Point Ground Flares: Predicted and Measured Flame Radiation in Cross Flow Wind Conditions," Sheraton Kauai Resort, Kauai, Hawaii, September 9 –11 (2016).

[8] C. Van Cauwenberge D.' C. Schietekat, J. Flore, V. G. V. and G. Marin, "CFD-based design of 3D pyrolysis reactors: RANS vs. LES," *Chemical Engineering Journal,* vol. 282, p. 66–76, 2015.

[9] J. Smith, B. Adams, R. Jackson and A. Suo-Antilla, "Use of RANS and LES Turbulence Models in CFD Predictions for Industrial Gas-fired Combustion Applications," *Journal of the International Flame Research Foundation,* no. Article number 201607, December 2017.

[10] R. Said, A. Garo and R. Borghi, "Soot Formation Modeling for Turbulent Flames," *Combustion and Flame,* vol. 108, pp. 71-86, 1997.

[11] B. Magnussen and B. Hjertager, "On Mathematical Models of Turbulent Combustion with Special Emphasis on Soot Formation and Combustion," *Sixteenth Symposium (International) on Combustion,* pp. 719-729, 1976.

[12] Y. Zhang, Hybrid Particle/Finite-Volume PDF Methods for Three-dimensional Time-Dependent Flows in Complex Geometries, State College, PA 16801: Department of Mechanical and Nuclear Engineering, Graduate School of Pennsylvania State University, 2004.

[13] D. J., R. B. and H. T., "Study of Quasi-Global Schemes for Hydrocarbon Combustion," *Combustion Science and Technology,* vol. 26, no. 1-2, pp. 1-15, 1981.

[14] K. I. K. and M. K., "A Numerical Study on Propagation of Premix Flames in Small Tubes," *Combustion and Flame,* vol. 146, pp. 283-301, 2006.

[15] J. Smith, R. Jackson, S. V. A. Suo-Anttila, D. Allen and S. Smith, " Withstanding the Wind," *Hydrocarbon Engineering,* vol. 21, no. 10, p. 43 – 49, October 2016.

[16] J. Smith, M. Henneke, C. Schnepper and M. Lorra, "Application of Computational Fluid Dynamics to Industrial Opportunities at the John Zink Company," in *Chemical Reaction Engineering VII: Computational Fluid Dynamics*, Quebec, Canada, August 6-11 (2000).